JOURNAL OF APPLIED ELECTROCHEMISTRY 17 (1987) 270–282

*Controlled nucleation and growth in chromium electroplating from molten LiCl–KCl**

T. VARGAS, D. INMAN

Department of Materials, Imperial College, London SW7 2BP, UK

Received 10 April 1986

The relationships between the electrochemical parameters (which can be controlled) and the resulting structures of chromium electrodeposits obtained by electrolysing chromous chloride ($CrCl_2$) dissolved in the LiCl–KCl eutectic have been established. The electrodeposition of chromium under ordinary potentiostatic conditions leads to pure chromium but this is not in a form to provide an adequate protective coating as it is difficult to avoid dendrite formation and low initial coverage together. These limitations can be overcome by the sequential use of a high overpotential pulse to initiate good coverage and continuing electrodeposition at low overpotential to minimize dendrite formation.

The structures and morphologies of chromium electroplates were optimized. The good protective coatings that resulted were adherent, coherent and reasonably free of cracks and pores. The macro- and microthrowing powers of the bath were excellent and the high purity of the chromium electroplates led to low (130–280 HV) measured microhardness.

1. Introduction

Many of the so-called refractory metals can only be electrodeposited in a pure form from non-protonic solvents such as molten salts. The advantages and disadvantages of these solvents have been described [1, 2]. Chromium is exceptional in this refractory metal group in as much as it can be electrodeposited from aqueous solution, albeit at low current efficiency. This arises from the co-deposition of hydrogen which can lead to poor quality electroplates containing cracks and pores [3]. However, in molten salt electrolytes, the presence of hydrogen/oxygen and other gases can be completely avoided which, in conjunction with the refining power of some baths, allows the electrodeposition of high purity chromium at efficiencies close to 100% [4]. In addition, better adherence of the deposits is likely in these baths because of the greater rates of intermetallic diffusion which are possible at high temperatures.

Several aspects of the electrodeposition of chromium from LiCl–KCl melts have already been studied. Electrochemical studies, carried out mainly in the LiCl–KCl eutectic, have generally focused attention on the characterization of the kinetics and mechanisms of the electroreduction [e.g. 5, 6]. Electrometallurgical studies of electrorefining have been directed towards obtaining a high-purity product, but no attempt has been made to control the morphologies of the deposits which have generally been highly dendritic [4, 7].

Recently we have studied the electrocrystallization mechanisms, identifying and characterizing the nucleation phenomena involved in the early stages of the electrodeposition of chromium on to foreign substrates [8–10]. In the present paper we establish the links between the (controlled) electrochemical parameters and the resulting structures of the chromium electrodeposits obtained from the LiCl–KCl eutectic, and describe our attempts to apply this funda-

* This paper was presented at a workshop on the electrodeposition of refractory metals, held at Imperial College, London, in July 1985.

0021–891X/87 $03.00 + .12

mental knowledge to a practical end, namely the optimization of the structures and morphologies desirable in electroplates which are to be used as protective coatings.

2. Experimental details

2.1. *Apparatus*

The electrochemical cell consisted of an outer Pyrex envelope (8 cm in diameter, 35 cm in height), at the bottom of which rested the vessel (6.5 cm in diameter, 17 cm in height) with the molten bath. The cell was capped by a water-cooled brass head designed to allow the introduction and interchange of electrodes, the feeding of chemicals, gas bubbling, etc., without contamination by the outside atmosphere. The cell, which could be operated under vacuum or purified argon, was placed in a temperature-controlled vertical furnace supplied from a Eurotherm unit.

For the generation of the different potential programmes a Wenking model PCA 72M (or L) potential control amplifier and a Princeton Applied Research model 175 universal programmer were employed in combination. Current transients were collected directly on a Bryans 2900 XY/t recorder, unless stored in a Datalab DL905 transient recorder as an intermediate stage.

The reference electrode, based on the Ag–0.5 M AgCl couple, consisted of a silver wire (Johnson Matthey, fine) immersed in a solution of AgCl (BDH Analar) in purified LiCl–KCl eutectic (see below) and contained in a pear-shaped glass bulb with a thin wall end [11]. The counter electrodes were made out of one or two chromium flakes (Halewood Chemicals Ltd, electrolytic, 99.999%) connected electrically with platinum–13% rhodium wire, forming an anode of 2–3 cm^2. The working electrodes were made out of commercial AGR fuel element cladding (double vacuum-melted, niobium-stabilized 20% chromium–25% nickel stainless steel) of 0.33–0.41 mm wall thickness, with one side presenting square ribs (0.23–0.31 mm) at 1.90–2.16 intervals. Flag microelectrodes were cut, giving rectangular edges with areas between 0.5 and 1.0 cm^2.

2.2. *Procedures*

The LiCl (BDH, anhydrous, GPR) and KCl (BDH, Analar) eutectic mixture (LiCl : KCl = 58.5 : 41.5 mol %) was purified initially according to a procedure of high vacuum desiccation at rising temperature until melting, chlorine bubbling, argon flushing, electrolysis and filtering [8]. Anhydrous $CrCl_2$ (Alfa Ventron, 98%), the source of chromium (II) ions, was used as obtained and added to the purified electrolyte in the cell before melting under vacuum. The electrochemical experiments were carried out under argon at a working temperature of 450° C.

The fuel cladding microelectrodes were previously treated anodically at room temperature in a solution of H_2SO_4 (specific gravity 1.53) applying 6 V with respect to a lead cathode for 1 min [12]. After electrodepositing in the molten bath the working electrodes were removed from the electrolytic cell (under positive argon pressure), immediately washed in running hot water to remove the melt retained on the surface of the deposit, rinsed in distilled water and acetone, and finally dried and kept in sealed flasks for examination. Scanning electron micrographs were obtained using a Joel Technics T200 or a Cambridge Stereoscan 600, scanning microscope. Optical micrographs were obtained using a Reichert Me/II inversion microscope which, for measurement of microhardness, was complemented by a Reichert microhardness tester.

3. Results and discussion

3.1. *Chromium electrogrowth at constant overpotential*

The results obtained in an initial experimental stage showed that the electrodeposition of chromium from $CrCl_2$–$(LiCl–KCl)_{eut}$ melts led, under simple potentiostatic conditions, to poor quality electroplates which are inadequate as protective coatings. This characteristic appeared under various depositing conditions, i.e. different chromium (II) ion concentrations and different depositing overpotentials. In general terms the electroplates presented either one, or a combination of, the following undesirable morphological characteristics: highly dendritic

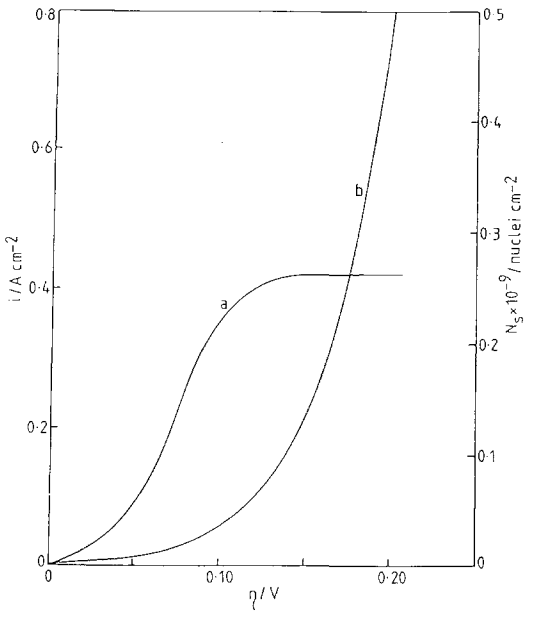

Fig. 1. Example of characteristic curves in the electrocrystallization of chromium under potentiostatic conditions on tungsten, when $C = 0.346\,\text{mol dm}^{-3}$. (a) Sampled current voltammogram (sampling time, 0.1 s); (b) saturation nucleus density versus overpotential.

structures, highly crystallized structures, incomplete coverage of the substrate, high structural interspace (voids) and poor adherence. The manifestation of each of these features varied from one deposit to another, according to the specific electrodepositing conditions used.

The variety of morphological features found in the chromium electroplates can be easily explained by the complex natures of the electrocrystallization phenomena at the early stages of electrodeposition on a foreign substrate. In the present case, this is found to be determined by two opposing aspects, i.e. the mechanism of the formation of the chromium phase on the foreign substrate and the characteristics of the electrochemical reduction of chromium (II) ions to chromium (0) itself. On the one hand, the early stages of the electrocrystallization of chromium in the present system involve a well defined, three-dimensional nucleation stage which has already been characterized [8–10]. Under potentiostatic conditions and after an initial induction period this process begins with the simultaneous formation and growth of three-dimensional chromium nuclei; the number of nuclei reaches a final saturation density well before the complete coverage of the electrode surface is attained and the final number is dependent on the chromium (II) ion concentration and the overpotential applied. On the other hand, the electroreduction of chromium (II) ions to the metal appears to be diffusion-controlled [9] as often occurs with electrode reactions in molten salts.

The main characteristics of the two aspects mentioned above may be summarized for the electrocrystallization of chromium on foreign substrates by the particular curves shown in Fig. 1 [8]. According to these curves and their relative positions, the difficulties encountered in producing coherent chromium electroplates under potentiostatic conditions can be explained in the following way. With respect to the electronucleation process, the electrodeposition of chromium at higher overpotentials is found to be better. In this case a higher saturation nuclei density is reached (curve b) and therefore a better initial coverage of the surface is obtained. Nevertheless, as the overpotential increases, the current becomes more diffusion-controlled, eventually reaching the limiting current level (curve a). This fact, in conjunction with the initial island growth, creates optimum conditions for the development of dendritic configurations [13]. The initially-formed crystallities which start growing with a current controlled by hemispherical diffusion, eventually develop preferentially in the direction of the solution bulk which provides a better supply of chromium (II) ions. At the same time, growth of nuclei in the horizontal direction is inhibited as the concentration of chromium (II) ions in the internuclei melt gradually decays. Fig. 2 illustrates this case, showing a chromium electrodeposit with the typical dendritic growth developed out of initially-formed nuclei.

With respect to the characteristics of the polarization curve (curve a, Fig. 1), electrodeposition at lower overpotential is advisable. As the deposition occurs in a region far from the limiting current, the diffusional overpotential becomes less important and the development of dendritic growth can be hindered, or at least delayed, for a longer time [13, 14]. Nevertheless, as the overpotential is lowered, the final saturation nuclei density drastically decreases and a

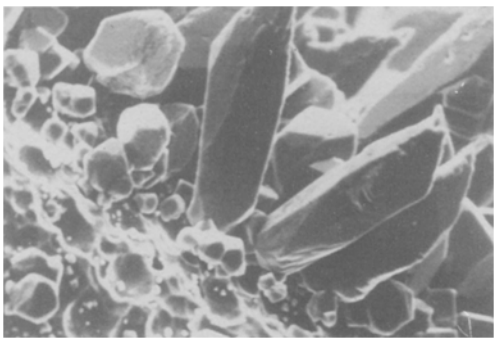

Fig. 2. Typical dendritic formations obtained in chromium electrodeposits. Dendritic deposit; $C = 0.354\,\text{mol}\,\text{dm}^{-3}$; $\eta = -0.85\,\text{V}$.

lower degree of coverage of the substrate is reached initially. Within the range of overpotentials before reaching the limiting current region, the initial degree of coverage is too low, the internuclei distance too great and the deposit does not reach a continuous structure. This situation is clearly shown in the structure of the chromium deposit shown in Fig. 3. The growth at lower overpotentials has effectively prevented the development of dendrites, and the deposit appeared as a continuous growth to the naked eye. However, the scanning electron micrographs show that the deposit is not compact, but is just the result of the growth of the initially-formed nuclei which have overlapped. The deposit has a high level of intercrystalline space (Fig. 3a) and there is a significant proportion of substrate area still uncovered (Fig. 3b).

From the relative positions of curves a and b in Fig. 1, it can be seen that there is no intermediate overpotential range where both phenomena can be prevented, i.e. dendrite formation and low initial coverage. Also, a change in chromium (II) ion concentration does not help in this situation as both limitations will be displaced in similar directions. For instance, an increase of concentration will result in a higher limiting current and a relatively larger overpotential range will be available for deposition without dendritic formation. However, as has been shown before [10], an increase in concentration also results in a decrease of the saturation nuclei density number, at the same time reducing the possibility of good coverage.

3.2. *Chromium electrogrowth using the initial potential pulse method*

Given the intrinsic characteristics for the growth of chromium electrodeposits at constant overpotential, which prevents the production of compact structures, an alternative method is now proposed and described in some detail. In this method the conditions for deposition in the early stages of formation of the deposit are different from the conditions used during the further growth and build-up of the macrodeposit.

A scheme of the basic programme of overpotentials proposed is shown in Fig. 4. First, a large overpotential pulse (or pulses), η_N, is applied for a length of time, t_N. During this stage the deposition occurs mainly through nucleation, and a high overpotential is used in order to reach a high saturation nuclei density which results in good initial coverage of the substrate. Immediately after the initial pulse the overpotential is

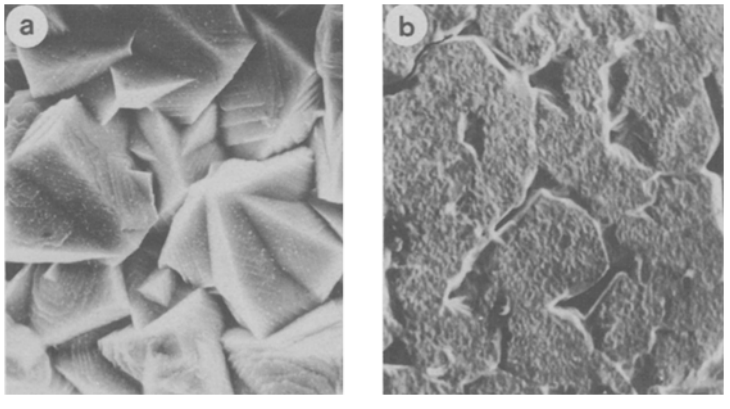

Fig. 3. Chromium electrodeposits obtained at low growth overpotential ($\eta = -0.03\,\text{V}$) and low chromium (II) ion concentration ($C \sim 0.14\,\text{mol}\,\text{dm}^{-3}$). (a) × 265; (b) × 160.

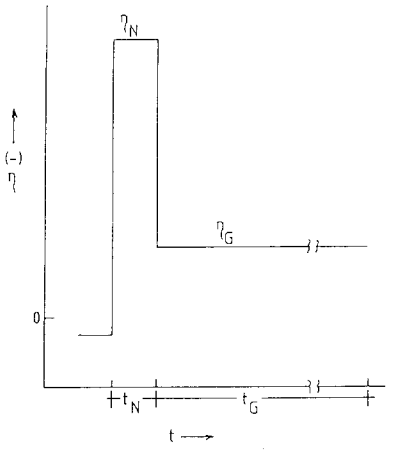

Fig. 4. Basic step waveform corresponding to the initial pulse method.

lowered to a value, η_G, which is applied for a time, t_G, long enough to build up the desired thickness. During this stage, deposition occurs mainly by the growth of the nuclei formed during the initial pulse. A conveniently low overvoltage is used at this stage in order to prevent the growth of dendrites and to create more favourable conditions for the coalescence of the nuclei into a continuous deposit.

The improvement of the morphological characteristics of chromium electrodeposits obtained when using an initial overpotential pulse is well illustrated in the scanning micrograph series shown in Fig. 5. In the case of an electrodeposit obtained at constant overpotential, the deposition is restricted to the growth of the few nuclei formed initially (Fig. 5a). Later in the process some of the nuclei have merged into a continuous layer but, because of the large initial internuclei distances, some interstitial zones where chromium is not deposited certainly remain (Fig. 5b). Electrodeposition carried out under similar conditions but with the introduction of three initial high overpotential pulses, increases the nuclei coverage, thereby producing a more even distribution of the chromium and a deposit which covers the substrate fully (Fig. 5c).

It is interesting to define the effect of the number of initial pulses on the morphology. Fig. 6 shows the morphology of chromium electrodeposits obtained when using different numbers of nucleation pulses. The deposits in Fig. 6a and b were obtained under the same conditions by using one and three pulses, respectively. When more than one pulse was applied a rest

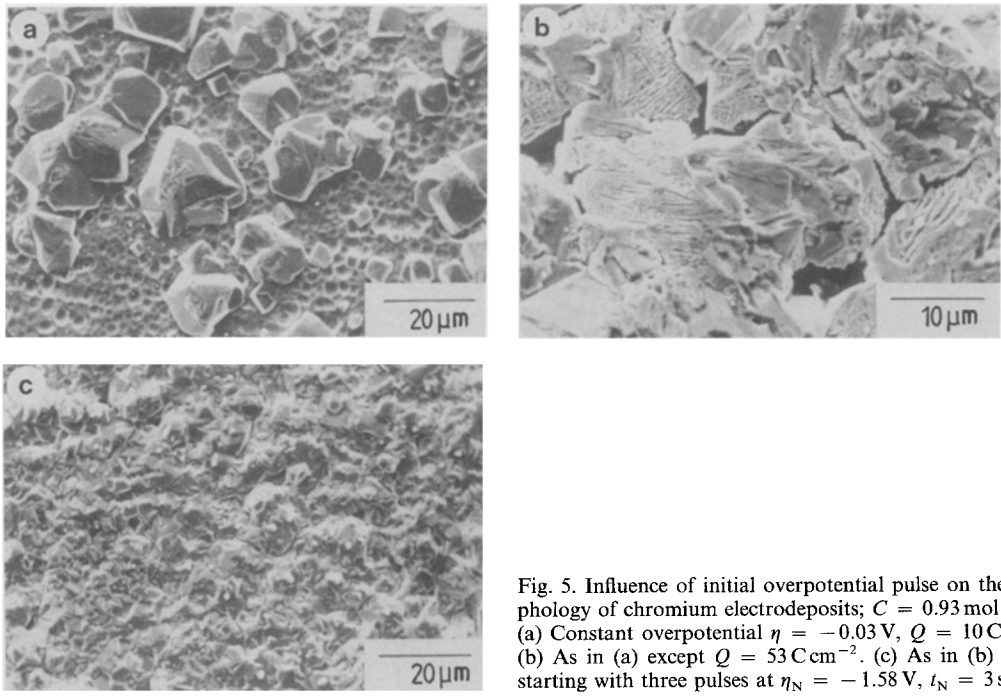

Fig. 5. Influence of initial overpotential pulse on the morphology of chromium electrodeposits; $C = 0.93\,\text{mol dm}^{-3}$. (a) Constant overpotential $\eta = -0.03\,\text{V}$, $Q = 10\,\text{C cm}^{-2}$. (b) As in (a) except $Q = 53\,\text{C cm}^{-2}$. (c) As in (b) except starting with three pulses at $\eta_N = -1.58\,\text{V}$, $t_N = 3\,\text{s}$.

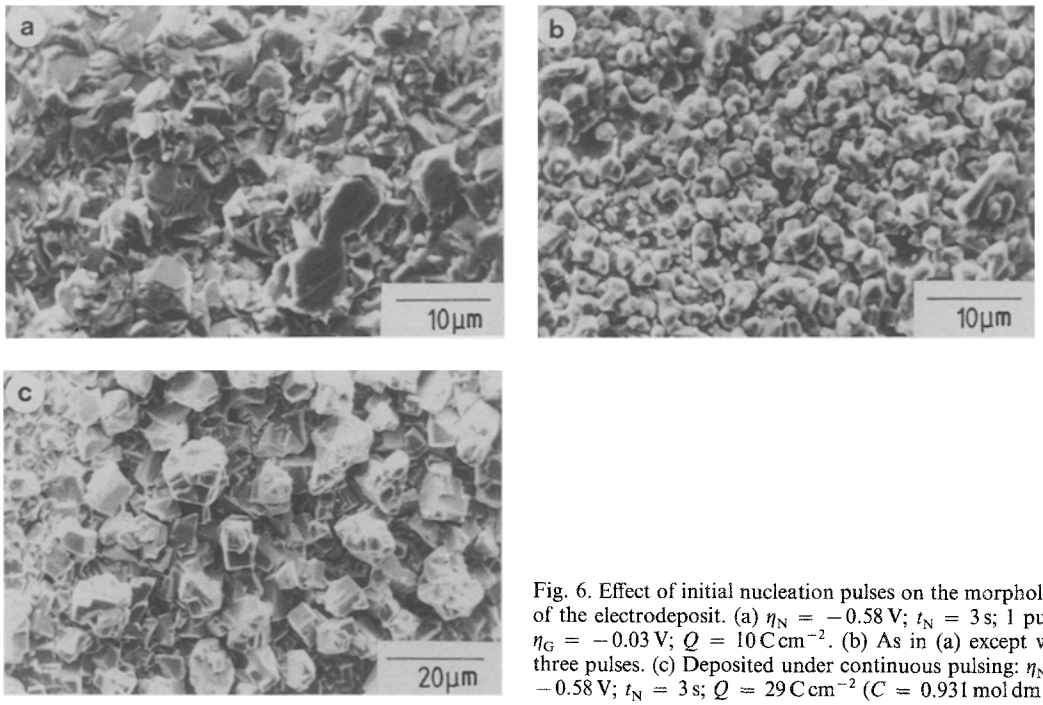

Fig. 6. Effect of initial nucleation pulses on the morphology of the electrodeposit. (a) $\eta_N = -0.58\,V$; $t_N = 3\,s$; 1 pulse; $\eta_G = -0.03\,V$; $Q = 10\,C\,cm^{-2}$. (b) As in (a) except with three pulses. (c) Deposited under continuous pulsing: $\eta_N = -0.58\,V$; $t_N = 3\,s$; $Q = 29\,C\,cm^{-2}$ ($C = 0.931\,mol\,dm^{-3}$).

time was left between each pulse. This is necessary to homogenize the chromium (II) ion concentration in the electrode vicinity (see Fig. 7a). The deposit in Fig. 6c was obtained under a continuous overpotential pulse–rest cycle (see Fig. 7b). It can be seen that the repetition of the initial nucleation pulse neither improves the coverage provided by the first overpotential pulse nor results in a better distribution of the chromium. Apparently the extra pulses enhance the growth of the initially formed nuclei, but no major extra deposition in the internuclei zones seems to occur. This behaviour can be explained by reference to the inhibitory action which growing chromium nuclei exert on nucleation, a phenomenon which has previously been analysed (10). In other words, as an initial number of nuclei has been formed during the first pulse, the application of additional overpotential pulses will result in the rapid growth of nucleation exclusion zones round the initially-formed nuclei. These then completely cover the internuclei area, preventing the onset of secondary nucleation processes and the improvement of the initial coverage. If the cycle overpotential pulse–rest (Fig. 7b) is repeated continuously, the substrate surface is eventually covered, but the deposition is not even and the initial nucleated morphology is maintained well into the process (Fig. 6c).

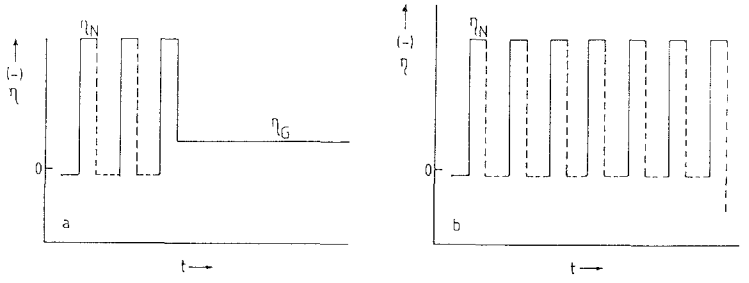

Fig. 7. Other step waveforms applied in the electrodeposition of chromium. (a) Three initial nucleation pulses; (b) continuous pulsing (the broken line indicates open circuit).

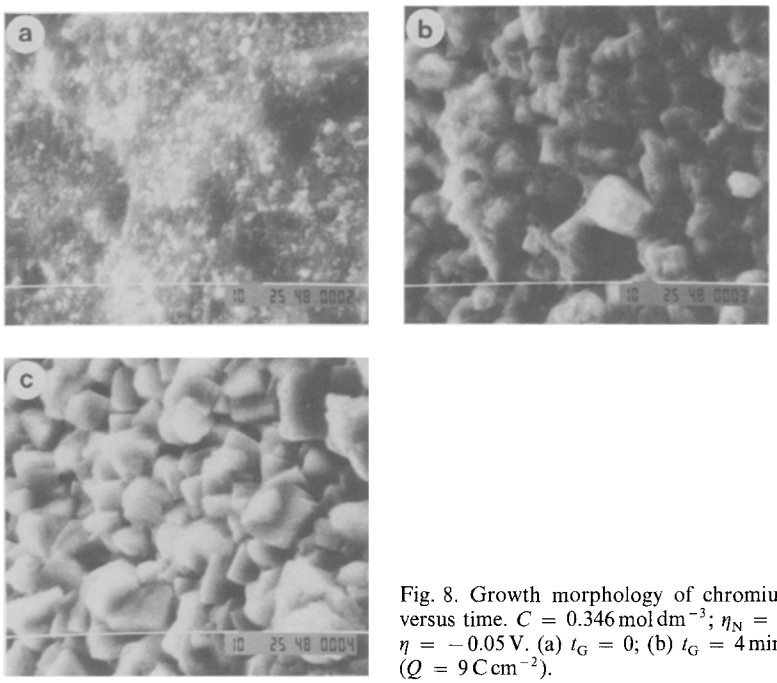

Fig. 8. Growth morphology of chromium electrodeposits versus time. $C = 0.346\,\text{mol}\,\text{dm}^{-3}$; $\eta_N = -0.6\,\text{V}$; $t_N = 1\,\text{s}$; $\eta = -0.05\,\text{V}$. (a) $t_G = 0$; (b) $t_G = 4\,\text{min}$; (c) $t_G = 21\,\text{min}$ ($Q = 9\,\text{C}\,\text{cm}^{-2}$).

The chromium (II) ion concentration plays a dual role in the mechanism of electrogrowth and it is necessary to define its influence. Given an initial nucleation pulse of a certain overpotential value, a higher initial nuclei saturation number will be reached if a lower chromium (II) ion concentration is used. However, although the use of low solute concentrations is advisable with regard to the initial coverage of the substrate, it is a disadvantage in the second stage of growth at low overpotential. Fig. 8 shows the evolution with time of the morphology of chromium electrodeposits obtained at relatively low chromium (II) ion concentrations. It can be seen that the use of an initial overpotential pulse produces a good initial coverage of the substrate with chromium nuclei. However, as the process continues, the deposits evolve into a structure consisting of discrete crystals which has a high degree of interspace and does not constitute a coherent protective layer. The formation of crystallized chromium deposits becomes especially noticeable when electrodepositing chromium at very low chromium (II) ion concentrations (Fig. 3a), and can be explained in terms of a low deposition–surface diffusion rate ratio. At low chromium (II) ion concentrations only a very small range of overpotential growth is available as the limiting current is low. Under these circumstances the electrodeposition rate is very low and the electrogrowth occurs close to equilibrium conditions. At the same time, a high surface diffusion rate is expected in a system at this temperature [15, 16] and therefore during the deposition there is enough time for the freshly deposited adatoms to migrate on the surface and find equilibrium sites corresponding to the crystal structure of chromium. This process is particularly easy to detect in the scanning micrograph in Fig. 3a where the growth steps of the chromium crystal are well defined.

At higher chromium (II) ion concentrations the lower saturation nucleus density obtained decreases the initial coverage of the substrate, but this situation is compensated for by the improvement in the characteristics of the low overpotential growth step. At higher chromium (II) concentration the electrocrystallization occurs at higher deposition rates and therefore the possibility for the growth of discrete crystals of chromium is reduced. This behaviour is well illustrated in the scanning micrograph sequence in Fig. 9 which shows the evolution with time of a chromium electrodeposit obtained in melts

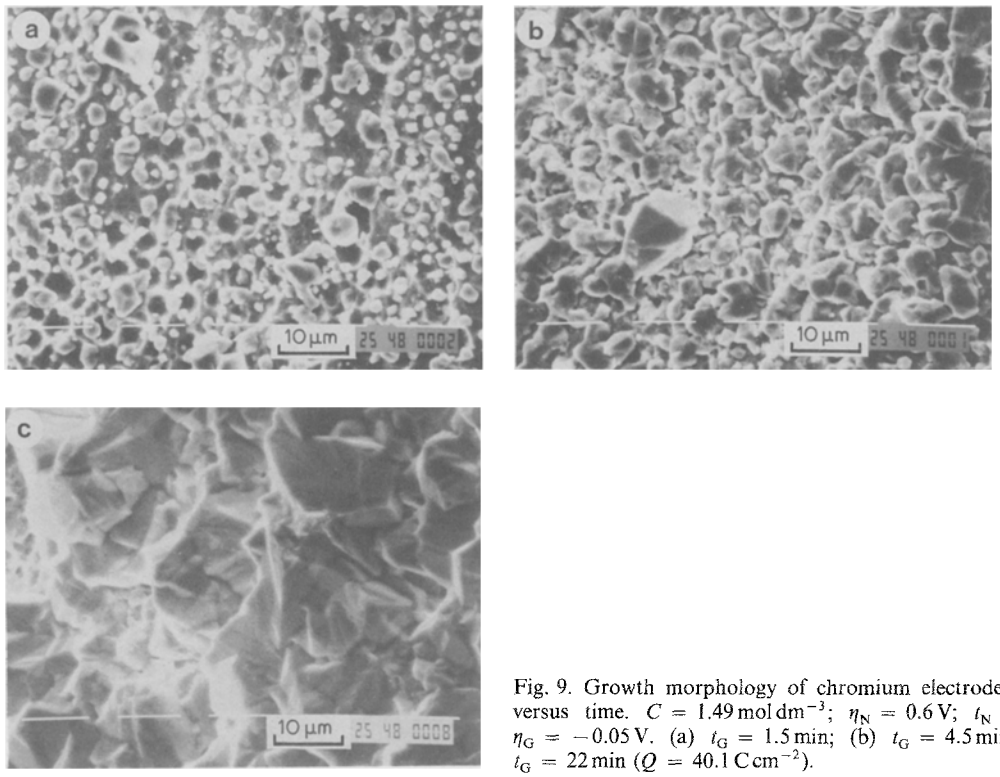

Fig. 9. Growth morphology of chromium electrodeposits versus time. $C = 1.49\,\text{mol dm}^{-3}$; $\eta_N = 0.6\,\text{V}$; $t_N = 1\,\text{s}$; $\eta_G = -0.05\,\text{V}$. (a) $t_G = 1.5\,\text{min}$; (b) $t_G = 4.5\,\text{min}$; (c) $t_G = 22\,\text{min}$ ($Q = 40.1\,\text{C cm}^{-2}$).

with $C = 1.49\,\text{mol dm}^{-3}$. The electrodeposition conditions used here are the same as those corresponding to Fig. 8, with the exception of the concentration change. It can be seen that at high chromium (II) concentration the nuclei grow in the form of rounded geometries and, even if the nuclei density number is initially lower, they eventually merge into a continuous layer. The morphology of the surface of the deposit after 22 min of deposition (Fig. 9c), however, still shows the formation of discrete crystals, a feature also noted in electrodeposits obtained at other solute concentrations; this indicates the strong tendency for this phenomenon to occur during the electrocrystallization of chromium in the present system. After the initial nucleation pulse is applied, the overpotential is set to a lower value where there are better conditions for the transition from the initial nuclei-dominated deposit into a continuous deposit. The use of a low overpotential in this stage is necessary to reduce the diffusion polarization round the growing nuclei, preventing their evolution into dendrites. At the same time a low overpotential is necessary to minimize the trapping of melt in the internuclei space, thus favouring the merging of the isolated nuclei. This factor can be better explained by reference to the schemes of growth morphology in Fig. 10. On the one hand, at the overpotential η_{G1}, the nuclei, growing under hemispherical diffusion control, develop preferentially in the direction of the bulk of the melt which provides a good supply of chromium (II) ions; the growth in the internuclei space decreases owing to the poor supply of solute and eventually the internuclei melt can be trapped if the nuclei frontal surfaces merge into a continuous front. On the other hand, at a conventiently low overpotential ($\eta_{G2} < \eta_{G1}$), surface control predominates and the diffusion layer round each nucleus is stationary or grows very slowly; the nuclei grow at the same rate in all directions and the melt in the internuclei space can eventually be displaced by the moving front of the deposit.

Considering the complexity of the transition stage of growth, it is difficult to recommend *a priori* an optimum value of growth overpotential to be used. However, a useful criterion was simply

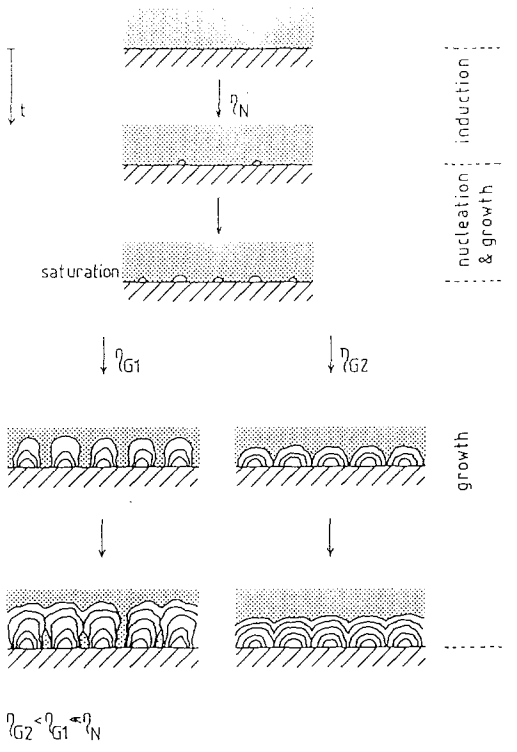

Fig. 10. Schematic representation of the morphological evolution of chromium electrodeposits at different growth overpotentials.

obtained from microscopic observations on chromium electrodeposits obtained under varying growth conditions. The electron scanning micrographs in Fig. 11 show the morphologies of chromium electrodeposits obtained at a high chromium (II) ion concentration (1.49 mol dm^{-3}), applying the same initial nucleation pulse but grown under different overpotentials. The sequence illustrates well the effect of the growth overpotential on the resultant morphology, showing the transition from a relatively even surface to a practically dendritic one as the overpotential increases in the range -0.2 to -0.1 V. This morphological evolution with increasing overpotential also evinces the corresponding increase of concentration polarization round chromium nuclei growing under hemispherical diffusion control, leading eventually to the preferential development of some nuclei at the expense of others which are deprived of solute. According to the results shown in Fig. 11, the development of protuberances can be qualitatively hindered only at very low growth overpotentials, say under -50 mV, when isolated nuclei merge into a coherent deposit. However, even if the growth of con-

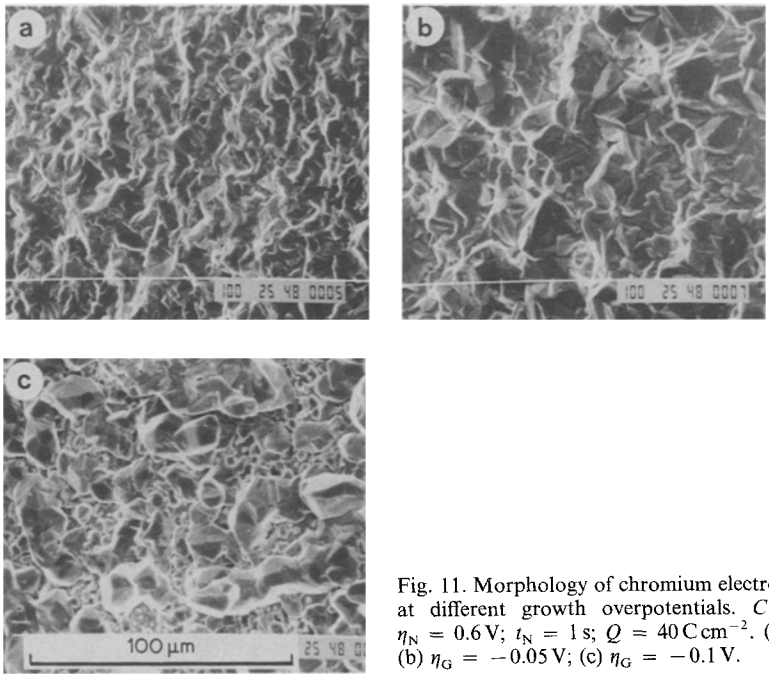

Fig. 11. Morphology of chromium electrodeposits obtained at different growth overpotentials. $C = 1.49$ mol dm^{-3}; $\eta_N = 0.6$ V; $t_N = 1$ s; $Q = 40$ C cm^{-2}. (a) $\eta_G = -0.02$ V; (b) $\eta_G = -0.05$ V; (c) $\eta_G = -0.1$ V.

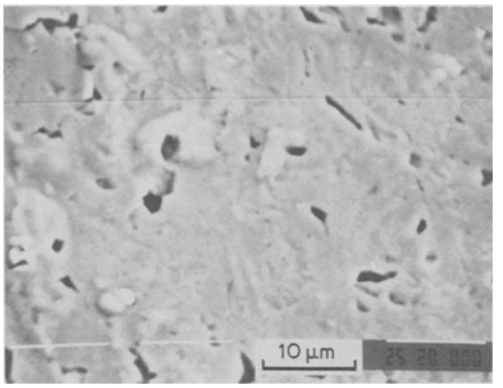

Fig. 12. Scanning electron micrographs of the back surface of chromium electrodeposits. $C = 1.61\,\text{mol dm}^{-3}$; $\eta_N = -0.6\,\text{V}$; $t_N = 0.5\,\text{s}$; $\eta_G = -0.05\,\text{V}$.

tinuous deposits is attainable at sufficiently low growth overpotentials, stricter conditions are apparently necessary to completely suppress the phenomenon of melt trapping in the nuclei interspace. The scanning electron micrographs in Fig. 12 show the morphologies of the back surfaces of chromium electrodeposits; that is, the surface which is in contact with the substrate. The small holes or gaps in the surface correspond to internuclei areas of the substrate which were not covered during the subsequent stage of growth of the deposit. The gaps in the substrate coverage correspond to points where the melt, after being depleted of chromium (II) ions, remained trapped in the structure of the deposit. Considering the low growth overvoltages used, it is difficult to prevent completely the occurrence of this phenomenon unless strong stirring is introduced in order to improve the supply of solute to the internuclei space.

3.3. *The production of protective chromium coatings using the initial potential pulse method*

Using the observed characteristics of the electrogrowth of chromium by the initial pulse method, criteria to select optimum operational parameters can be defined under the following headings. (i) Use of high chromium (II) ion concentrations, preferably over $1\,\text{mol dm}^{-3}$. (ii) Use of a nucleation overvoltage, η_N, as high as possible; its highest value will be limited by the decomposition voltage of the melt and a typical

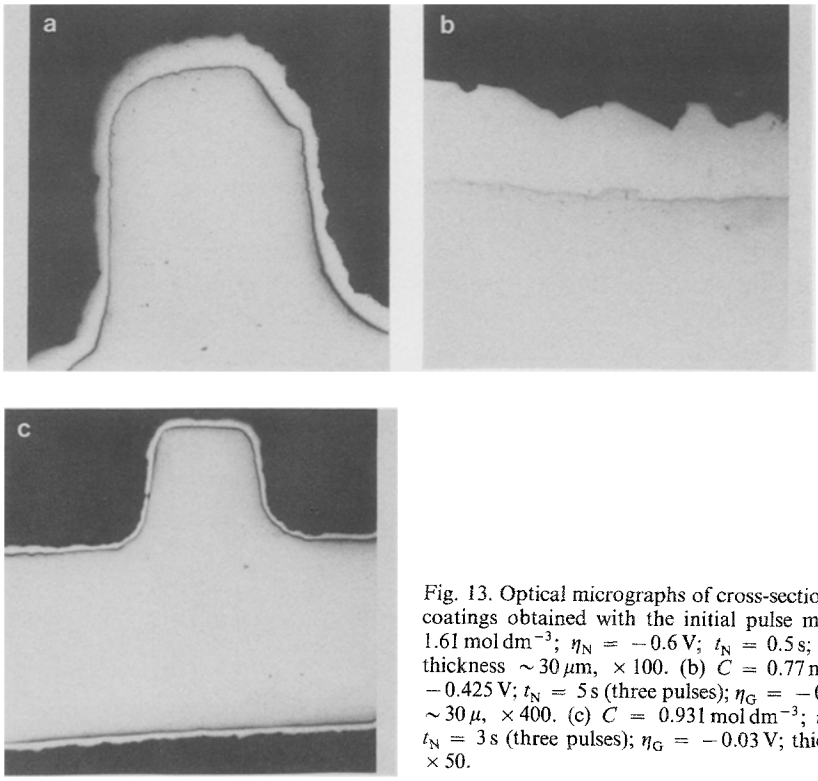

Fig. 13. Optical micrographs of cross-sections of chromium coatings obtained with the initial pulse method. (a) $C = 1.61\,\text{mol dm}^{-3}$; $\eta_N = -0.6\,\text{V}$; $t_N = 0.5\,\text{s}$; $\eta_G = -0.05\,\text{V}$; thickness $\sim 30\,\mu\text{m}$, $\times 100$. (b) $C = 0.77\,\text{mol dm}^{-3}$; $\eta_N = -0.425\,\text{V}$; $t_N = 5\,\text{s}$ (three pulses); $\eta_G = -0.03\,\text{V}$; thickness $\sim 30\,\mu$, $\times 400$. (c) $C = 0.931\,\text{mol dm}^{-3}$; $\eta_N = -0.58\,\text{V}$; $t_N = 3\,\text{s}$ (three pulses); $\eta_G = -0.03\,\text{V}$; thickness $\sim 20\,\mu\text{m}$, $\times 50$.

Table 1. Some typical working conditions used in the production of chromium coatings on niobium-stabilized 20/25 stainless steel probes

	A	*B*	*C*	*D*
Temperature, °C	450	450	450	450
C, mol dm^{-3}	0.77	0.93	1.49	1.61
Nucleation overpotential, mV	−425	−600	−600	−600
Nucleation time, s	5	3	0.5	0.5
No. of nucleation pulses	2	3	1	1
Growth overpotential, mV	−35, −40	−50	−50	−40
Growth current density, mA cm^{-2}	14–16	17–18	29–30	19–20
Final deposit thickness, μm	30–35	20–30	30	30

practical range is between −0.5 and −1.0 V. (iii) Use of a nucleation pulse length t_N which is long enough to attain the saturation nucleus density but short enough to prevent an excessive growth of the nuclei at this overpotential; a value of t_N in the range 100 μs to 1 s is considered adequate. (iv) Use of a growth overpotential, η_G, no greater than 50 mV unless stirring of the melts is introduced. A more general account of the method can be found in [17].

Using these criteria, chromium electroplating was attempted using the different experimental conditions which are summarized in Table 1.

Fig. 13 shows the typical morphological characteristics of the deposits obtained. The chromium forms a deposit which is coherent, free of cracks and pores, and which fully covers the substrate surface.

The X-ray diffraction pattern of the deposited chromium indicated a body-centred cubic lattice which corresponds to the stable form of chromium [18]. A quantitative evaluation of the purity of the chromium deposit using a microprobe analysis technique (Joel T-200 SEM) revealed only the peaks corresponding to chromium [19]. The chromium coatings present, in general, a rather uneven external surface as is clearly seen in the cross-section shown in Fig. 13c. This characteristic corresponds to the crystalline features of the surface of chromium coatings revealed in the scanning electron micrographs shown above (Fig. 9c). This characteristic could be improved if the process of electrodeposition was carried out in conditions where the development of the crystalline features of the deposit surface could be inhibited. This could be achieved by introducing stirring of the electrolytic bath, making possible the application of higher growth overpotentials and higher electrodeposition rates. (It was not possible to attempt the use of stirring in the present experiments which were all carried out in a small electrolytic cell.) Electrodeposition under potential reversal conditions, a method which has proved advan-

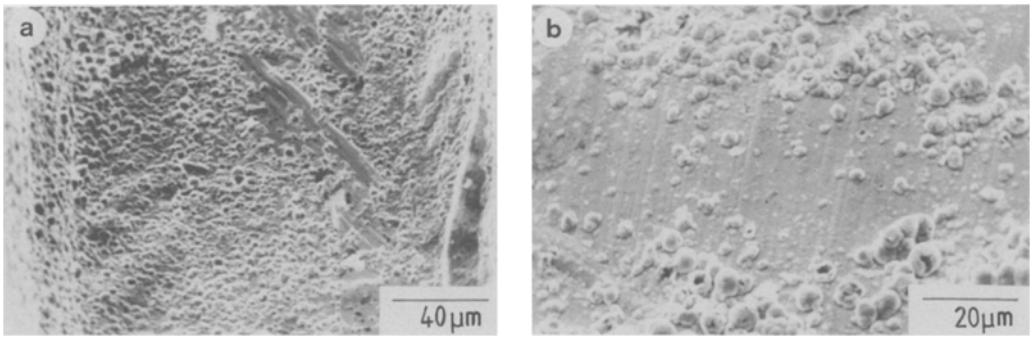

Fig. 14. (a) Typical features obtained on the surface of 20/25 niobium stabilized stainless steel probes after anodic etching. (b) Typical features of the back surface of chromium coatings obtained on 20/25 niobium stainless steel probes.

tageous in applications in aqueous systems [20] can also, when applied at the growth stage, result in improved chromium deposit surfaces [19].

The cross-sections shown in Fig. 13a and c illustrate the characteristics of the distribution of the chromium deposit round the ribs on the fuel can probe. The thickness of the chromium coating is relatively constant all over the rib profile, indicating a good macrothrowing power. This in turn indicates an even current distribution on the cathode and suggests the predominance of a secondary current distribution which is expected in a bath where polarization predominates over ohmic effects [21]. The high efficiency of chromium deposition in this bath is a factor which also contributes to the good throwing power.

The microthrowing power is illustrated to some extent in the cross-section shown in Fig. 13b. The good contact existing all along the deposit–substrate interface shows the ability to cover homogeneously all the different microirregularities existing on the substrate surface. This feature, on a smaller scale, can be seen in Fig. 14a and b which show the typical morphologies of the etched probe surface and the particular surface of the chromium deposit in contact with it (back surface). The nodular morphology of the back surface of the coating has been determined by the pitted probe surface morphology showing how the deposited chromium has filled practically all these intricate microscopic irregularities. Nevertheless, by observing the microscopic gaps in the inner surface of the deposit (Fig. 12) one can see that there is still a small fraction of the substrate area where there is no deposit–substrate contact. The nature of this phenomenon was discussed above and interpreted in relation to the mechanism during the initial stages of electrocrystallization.

Microhardness measurements using a Vickers' instrument were performed on cross-sections of chromium coatings. The values of microhardness obtained were in the range of 130 to 280 HV, which is much lower than that obtained for chromium electrodeposits from aqueous solutions which are typically in the range of 850 to 1000 HV [22].

The low microhardness of the chromium obtained accords well with its high purity [23]. This good purity can easily be achieved with a molten bath free of the most typical impurities, i.e. oxygen and hydrogen, and also because of the refining properties which LiCl–KCl–$CrCl_2$ melts have in relation to chromium [4].

The adherence between the chromium coatings and the fuel can material was tested with a Sebastian adherence tester which led to the conclusion that the chromium-coating, 20/25 niobium stainless steel adherence was greater than 240–250 kgf cm^{-2}. The good chromium adherence is also an expected property when depositing from molten salts and is related to the ability of these media to dissolve any oxide film or moisture film remaining from the substrate surface [24]. In the present case it can also be related to the method of electrodeposition used which, introducing an initial nucleation pulse, resulted in the attainment of an improved microthrowing power and then an intimate contact between the coating and the substrate. At the same time the bond between the chromium and the substrate obtained in the present system appears to be quite strong in itself, as deduced from the characterization of adherence in the electronucleation studies [8]. In addition, the initial strength of this link is expected to increase during the process as a result of interdiffusion, a phenomenon which has been found to occur to some extent in this system when depositing chromium on low-carbon steel [19].

4. Conclusions

The involvement of a nucleus saturation mechanism in the electrocrystallization of chromium from the LiCl–KCl eutectic precludes the ready transition from island to continuous growth, making it impossible in practice to obtain a coherent electrodeposit under simple potentiostatic conditions. This intrinsic disadvantage is overcome by using an initial potential pulse method which substantially improves the electrogrowth of chromium.

This method has been found to be the best way of electrodepositing chromium from this melt, allowing the production of high-purity electroplates with low hardness, no cracks and good adherence, together with good coverage of the substrate. Tests performed on 20–25 stain-

less steel probes protected with such coatings indicated a good corrosion resistance against carbon deposition reactions at high temperatures [25].

Acknowledgements

The financial support for this work came from the CEGB. We are especially grateful to Dr M. P. Hill of that organization (CERL, Leatherhead) for valuable discussions and advice.

References

[1] D. Inman and S. H. White, *J. Appl. Electrochem.* **8** (1978) 375.
[2] R. S. Sethi, *ibid.* **9** (1979) 411.
[3] A. H. Sully, 'Metallurgy of the rarer metals – 1: Chromium'. Butterworths Scientific Publications, London (1954).
[4] K. P. V. Lei, J. M. Hiegel and T. A. Sullivan, *J. Less Common Metals* **27** (1972) 353.
[5] D. Inman, J. C. L. Legey and R. Spencer, *J. Electroanal. Chem.* **61** (1975) 289.
[6] R. E. Cains Jr. and N. J. Grant, *Trans. AIME* **230** (1964) 1156.
[7] A. K. Suri and C. K. Gupta, *Surf. Technol.* **5** (1977) 271.
[8] T. Vargas, PhD Thesis, Imperial College, London (1984).
[9] T. Vargas and D. Inman, to be published.
[10] T. Vargas and D. Inman, to be published.
[11] J. O'M. Bockris, G. J. Hills, D. Inman and L. Young, *J. Sci. Instr.* **33** (1956) 438.
[12] F. M. Dorsey, *Ind. Eng. Chem.* **20** (1928) 1094.
[13] A. R. Despic and K. I. Popov, in 'Modern Aspects of Electrochemistry', Vol. 7 (edited by B. E. Conway and J. O'M. Bockris), Butterworth & Co. Ltd, London (1972) p. 199.
[14] K. I. Popov, M. D. Maksimovic and J. D. Trnjancev, *J. Appl. Electrochem.* **11** (1981) 239.
[15] N. A. Gjostein, in 'Metal Surfaces', American Society for Metals, Metals Park, Ohio (1963) chap. 4.
[16] T. B. Reddy, *J. Electrochem. Soc.* **113** (1966) 117.
[17] M. P. Hill, D. Inman and T. Vargas, UK Patent Application No. 8403184, 8 Feb. 1984.
[18] A. H. Sully, 'Chromium Plating', Robert Draper, Teddington, Middlesex, UK (1954), chap. 3.
[19] D. Inman, T. Vargas, S. Duan and P. Dudley, in 'Proceedings of 4th Int. Symposium on Molten Salts', New Jersey, The Electrochemical Society Inc. (1984) pp. 545.
[20] A. R. Despic and K. I. Popov, *J. Appl. Electrochem.* **1** (1971) 275.
[21] F. A. Lowenheim, in 'Modern Electroplating', John Wiley & Sons Inc., New York (1974) chap. 1.
[22] P. Morriset, J. W. Oswald, C. R. Draper and R. Pinner, 'Chromium Plating', Robert Draper, Teddington, Middlesex, UK (1954).
[23] A. Brenner, P. Burkhead and C. Jennings, *J. Res. Nat. Bur. Standards* **40** (1948) 31.
[24] J. Wurm, *Met. Finish.* **78** (1980) 37.
[25] M. P. Hill, private communication (and see *J. Appl. Electrochem.* **17** (1987) 283.